^{19}F nuclear magnetic resonance studies of $KCoFeF_6$: a geometrically frustrated system

1999 J. Phys.: Condens. Matter 11 4261

(http://iopscience.iop.org/0953-8984/11/21/312)

J. Phys.: Condens. Matter **11** (1999) 4261–4274. Printed in the UK PII: S0953-8984(99)00011-9

^{19}F nuclear magnetic resonance studies of $KCoFeF_6$: a geometrically frustrated system

S Giri, K Ghoshray† and A Ghoshray

SS&MP Division, Saha Institute of Nuclear Physics, 1/AF Bidhannagar, Calcutta 700 064, India

E-mail: kgr@cmp.saha.ernet.in

Received 8 December 1998, in final form 22 March 1999

Abstract. ^{19}F nuclear magnetic resonance (NMR) studies are performed on polycrystalline $KCoFeF_6$ for temperatures in the range T_N (110 K) $< T \leqslant 400$ K. The transferred hyperfine interaction parameters K_{iso} and K_{ax} are determined at 294 K for the eight types of fluorine present in the unit cell. The results give an idea of the variation of the M–F bond lengths for different F^- ions. The fractional spin transfer from the 3d to the 2s orbitals of the different F^- ions has also been estimated. The temperature dependence of K_{iso} suggests the absence of the development of any short-range antiferromagnetic correlations within the magnetic ions bonded on either side of each type of F^- ion, even very close to T_N, whereas the temperature dependence of K_{ax} suggests an appreciable enhancement of the anisotropic part of the hyperfine field below 160 K. Moreover, the intrinsic linewidths of the constituent lines increase appreciably below the same temperature, where the bulk susceptibility does not show such extra enhancement. This feature resembles the effect of slowing down of electron spin fluctuations on the ^{19}F NMR linewidth. A comparison of the behaviour of the shift parameters with those found for $KMnFeF_6$ indicates the dominance of geometrical frustration within the magnetic ions in the triangular lattice over the tendency of magnetic ordering of the ions belonging to the square lattice in the paramagnetic phase in $KCoFeF_6$.

1. Introduction

Study of cooperative phenomena in magnetism has provided a useful testing ground for theories of interacting systems which possess different spatial dimensions, ranges, and signs of interactions, and that exhibit local anisotropy of spin. Moreover, the competition among two-body interactions in a Bravais lattice yields a large variety of ground states. Various classes of magnets are defined by the nature of this competition—for example, multisublattice antiferromagnetism, ferrimagnetism, metamagnetism. In the past few years, a class of materials which display a distinct type of competition and related low-temperature behaviour not yet seen in any other magnetic systems has been recognized [1]. They represent the extreme cases of antiferromagnets where the total-energy minimum far exceeds the energy corresponding to minimizing each individual bond. These systems have been called the geometrically frustrated magnets [2], since the competition among nearest-neighbour spins arises from the shared property of triangular site coordination. For these systems the features of the thermodynamic and spectral response below T_c are rather unusual and are not yet understood.

The present paper reports the local magnetic properties of the compound $KCoFeF_6$ in which the geometrically frustrated triangular lattice coexists with the unfrustrated square lattice. This is a member of the isomorphous series with general formula $KMM'F_6$ (where

† Author to whom any correspondence should be addressed.

0953-8984/99/214261+14$19.50

M and M′ are divalent and trivalent transition metal ions respectively), and crystallizes in the tetragonal tungsten-bronze-type structure [3, 4]. The crystal structure projected along the *c*-axis is shown in figure 1. The magnetic behaviours of such compounds are determined by the superexchange interactions: M–F–M′, M′–F–M′, and M–F–M. The high-field dc susceptibility clearly shows a large negative value of the Curie–Weiss temperature: $\Theta \sim -440$ K and -420 K for $KMnFeF_6$ [5] and $KCoFeF_6$ [6] respectively. This suggests the presence of strong antiferromagnetic (AF) exchange in the lattice. Thus in this type of structure, strongly frustrated triangular platelets of magnetic ions should coexist with the unfrustrated square platelets which would favour long-range order.

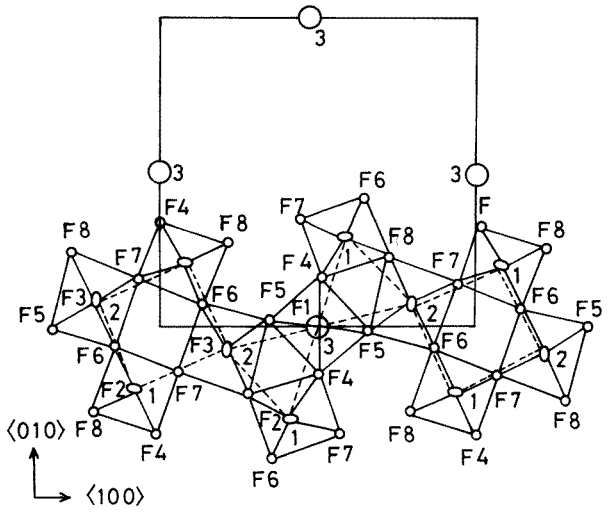

Figure 1. A portion of the metal–fluorine network projected along the ⟨001⟩ direction. Transition metal sites 1, i.e., M(1), 2, i.e., M(2), and 3, i.e., M(3), are occupied by Mn^{2+}, Fe^{3+}, and—statistically—Mn^{2+}/Fe^{3+}, respectively. Magnetic ions in the triangular cycles and square platelets are shown by dashed lines. Fluorine ions F1–F8 correspond to F(1) to F(8) respectively, as mentioned in the text.

In the case of $KMnFeF_6$, both χ_{dc} [5] and χ_{ac} [7] show a sharp increase at 148 K (T_N), indicating the appearance of a ferrimagnetic-type ordering. However, near 133 K both the real (χ') and imaginary (χ'') parts of χ_{ac} decrease sharply, with the result that there is a very sharp peak at 133 K. Moreover, a very broad peak appears in both χ' and χ'' near 108 K with considerable distribution in the internal magnetic fields over the temperature range $108\ \text{K} \leqslant T \leqslant 148\ \text{K}$ (T_N) as is evident from Mössbauer data [7]. In contrast, χ_{dc} maintains its increasing trend below 148 K, like a ferrimagnet. On the other hand, in the case of $KCoFeF_6$ the χ_M^{-1}–T curve [6] shows a very broad upward cusp at around 110 K (T_N), indicating the predominance of short-range AF order near T_N. However, χ' in this case shows a very sharp peak at 110 K indicating an AF-type ordering. Moreover, there appears a non-zero value of the absorption part χ'' below T_N for $KCoFeF_6$, which increases continuously with further lowering of temperature down to ∼58 K [8]. The appearance of non-zero χ'' below T_N in this case indicates the presence of ferromagnetic (F) correlations below the AF ordering temperature [9].

These findings demand more experiments for comparison of the nature of the local magnetic ordering as a function of temperature for $KMnFeF_6$ and for $KCoFeF_6$ when they approach T_N from the paramagnetic phase. Moreover, substitution of Co^{2+} in place of Mn^{2+}

introduces the effect of single-ion anisotropy on the M–F–M′ superexchange interaction. As in these compounds the exchange interactions of the two transition metal ions are mediated via the ligand F^- ion, ^{19}F NMR studies would be very useful to probe the nature of the short-range magnetic correlations which are developed far above T_N. Such studies can directly probe, through ^{19}F NMR transferred hyperfine interaction parameters, hybridization of the 3d electrons with ligand electron orbitals, which plays a dominant role in determining the nature of the local as well as the bulk magnetic ordering of such systems.

Recently we have reported detailed ^{19}F NMR results for $KMnFeF_6$ [10, 11] for the temperature range $T_N < T \leqslant 395$ K. It has been shown that the spins in the triangular cycles of the magnetic ions start to be canted from ∼270 K, which is well above T_N (148 K), whereas those belonging to the square platelets favour antiparallel alignment below this temperature. Finally, the ^{19}F NMR line has been found to vanish at T_N (148 K), though the Mössbauer data [7], even below 100 K, do not correspond to a long-range-ordered state. In the present paper we report detailed ^{19}F NMR results for polycrystalline $KCoFeF_6$ for the temperature range T_N (110 K) $\leqslant T \leqslant 400$ K, and give a comparison with the results for $KMnFeF_6$ [10,11].

The methods of sample preparation were described earlier [6]. ^{19}F cw NMR studies are performed at resonance frequencies of 15 and 34 MHz using a Varian Associates WL210 nuclear induction spectrometer with a V7400 15 inch electromagnet. To increase the S/N ratio, a Tracor Northern NS5701A signal averager is incorporated. Shifts are measured with respect to the resonance frequency, ν_R, corresponding to the ^{19}F NMR line in an NH_4F solution.

2. Experimental results

2.1. NMR results at 294 K

Figure 2(a) shows the ^{19}F NMR spectra of $KCoFeF_6$ at 294 K at the resonance frequencies 15 MHz and 34 MHz. The same thing but at 31 MHz is shown in figure 2(b) for the case of isostructural $KMnFeF_6$ [10], for comparison. It may be seen that the substitution of Co^{2+} ($3d^7$) in place of Mn^{2+} ($3d^5$) does not affect the high-frequency part of the spectrum. However, a structure towards the low-frequency side appears in the case of $KCoFeF_6$. In both cases the whole spectrum is shifted towards the high-frequency side with respect to the reference (ν_R). Since there are eight types of fluorine in the unit cell of this type of compound (figure 1), the NMR spectrum would be a superposition of a number of resonance lines corresponding to the ^{19}F nuclei experiencing different local magnetic fields. In order to analyse this spectrum, we have to deconvolute the experimental line into different constituent lines having different parameters using the derivative of the equation [12]

$$I(\nu') = \int_{-\infty}^{\infty} p(\nu) \exp\left[-\frac{(\nu - \nu')^2}{2\beta^2}\right] \mathrm{d}\nu. \tag{1}$$

$I(\nu')$ represents the NMR line shape in a polycrystalline sample in the presence of an anisotropic internal field, superimposing a Gaussian broadening 2β on the resonance line from each of the crystallites. Here,

$$p(\nu) \sim 1/|\mathrm{d}\nu/\mathrm{d}(\cos\theta)|$$

where

$$\nu = \nu_1 \sin^2\theta \sin^2\phi + \nu_2 \sin^2\theta \cos^2\phi + \nu_3 \cos^2\theta$$

is the resonance frequency of a single crystal. θ and ϕ denote the direction cosines of the external magnetic field ($\boldsymbol{H}_0$) with respect to the principal axes of the electron nuclear magnetic coupling tensor. ν_1, ν_2, ν_3 are frequencies at which the resonances occur if $\boldsymbol{H}_0$ points along

one of the axes. It is assumed that $\nu_1 < \nu_2 < \nu_3$. The frequencies ν_1, ν_2, ν_3 are related to the principal components, K_1, K_2, K_3, of the total (dipolar and hyperfine) shift tensor as follows: $\nu_i = \nu_R(1 + K_i)$ (i runs from 1 to 3), where ν_R is the position of the resonance line in the diamagnetic reference. So the expression for ν reduces to the form

$$\nu = \nu_R[1 + K_{iso} + K_{ax}(3\cos^2\theta - 1) + K_{aniso}\sin^2\theta\cos^2 2\phi] \tag{2}$$

where

$$K_{iso} = \frac{1}{3}(K_1 + K_2 + K_3) \qquad K_{ax} = \frac{1}{6}(2K_3 - K_1 - K_2) \qquad K_{aniso} = \frac{1}{2}(K_1 - K_2).$$

If the nucleus experiences an internal field of cylindrical symmetry, the third term K_{aniso} in the expression for ν vanishes, since $K_1 \approx K_2$. As in a polycrystalline specimen, the crystallites are oriented randomly, the deviation from cubic symmetry of the internal magnetic field leads to a broadening of the resonance line.

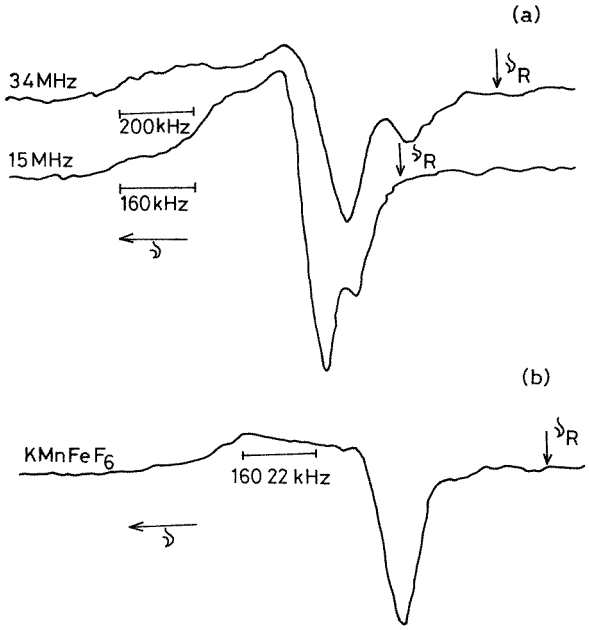

Figure 2. ^{19}F NMR spectra of (a) polycrystalline $KCoFeF_6$ at 294 K, at the resonance frequencies 15 and 34 MHz, and (b) $KMnFeF_6$ at 294 K, at the resonance frequency 31 MHz (reference [10]).

For unambiguous fitting of such a complex spectrum, it is necessary to have prior knowledge of some of the parameters. Two of them are the electron–nuclear dipolar contribution to the total shift parameters and the nuclear–nuclear dipolar interaction contributing to the linewidth ($\delta\nu_n$). Far above the magnetic ordering temperature, the intrinsic linewidth, 2β (equation (1)), is nearly equal to $\delta\nu_n$, since the electronic contribution is negligible due to the fast flipping of the spins. Both the dipolar shift parameters and $\delta\nu_n$ can be estimated from the knowledge of the crystal structure. Calculation of $\delta\nu_n$ is straightforward, and the results are listed in table 1.

As may be seen from figure 1, most of the M–F–M bonds in this compound do not coincide with any one of the crystallographic axes; the calculated values of the dipolar-field components along these axes would, therefore, not be the principal components. The five

Table 1. Different types of fluorine, and their numbers within the unit cell (N), calculated principal components of the fractional dipolar shift, and the nuclear–nuclear dipolar contribution to the linewidth ($\delta\nu_n$), for the fluorines in the case of $KCoFeF_6$.

Fluorine	N†	Metal–fluorine bond direction	$\delta H_d/H_0$			K_{ax}^d (%)	K_{aniso}^d (%)	$\delta\nu_n$ (kHz)
			K_1' (%)	K_2' (%)	K_3' (%)			
F(1)	4	M(3)–F(1)–M(3)	−0.163	−0.236	0.399	0.199	0.036	26.6
F(2)	8	M(1)–F(2)–M(2)	−0.182	−0.224	0.406	0.203	0.021	27.8
F(3)	8	M(1)–F(3)–M(2)	−0.180	−0.221	0.401	0.200	0.020	28.4
F(4)	8	M(1)–F(4)–M(3)	−0.126	−0.276	0.407	0.201	0.074	40.7
F(5)	8	M(2)–F(5)–M(3)	−0.221	−0.316	0.537	0.268	0.047	31.8
F(6)	8	M(1)–F(6)–M(2)	−0.236	−0.279	0.515	0.258	0.021	27.8
F(7)	8	M(1)–F(7)–M(2)	−0.239	−0.285	0.524	0.262	0.022	27.8
F(8)	8	M(1)–F(8)–M(2)	−0.131	−0.281	0.412	0.206	0.075	27.6

† Reference [4].

independent components of the dipole-field tensor with respect to the crystallographic axes are then determined from the formula

$$H_{ij}^{D} = \sum \frac{3r^i r^j - r^2\delta_{ij}}{r^5}\langle\mu\rangle \qquad i, j = x, y, z. \tag{3}$$

Here $\langle\mu\rangle$ corresponds to the moment of the Co^{2+} ion for the M(1) site, the Fe^{3+} ion for the M(2) site, and the average of the moments of the Co^{2+} and Fe^{3+} ions for the M(3) site. Since the Fe^{3+} ions in $KMnFeF_6$ and $KCoFeF_6$ have similar crystallographic environments, $\langle\mu_j\rangle_{Fe^{3+}}$ may be assumed to be same in the paramagnetic state for the two cases. On the basis of this consideration, $\langle\mu_j\rangle_{Fe^{3+}}$ is calculated from the following relation:

$$\langle\mu_j\rangle_{Fe^{3+}} = \frac{\chi_M(\text{for } KMnFeF_6)H_R}{2N} \tag{4}$$

and $\langle\mu_j\rangle_{Co^{2+}}$ is then calculated by subtracting $\langle\mu_j\rangle_{Fe^{3+}}$ from $\langle\mu_j\rangle_{Co^{2+}} + \langle\mu_j\rangle_{Fe^{3+}}$ for $KCoFeF_6$. The estimated principal components of the fractional dipolar shift tensors (K_1', K_2', K_3') for eight types of fluorine are listed in table 1. It has been observed that for each of the fluorines, consideration of all of the neighbouring metal ions contained within a sphere of radius 50 Å is sufficient in the calculation of $\boldsymbol{H}_d$. From table 1 it is seen that the natures of the dipolar fields experienced by all of the fluorines in $KCoFeF_6$ are similar to that for $KMnFeF_6$, though the magnitudes of K_1', K_2', K_3' are smaller in the former case. This is consistent with the smaller values of $\langle\mu\rangle_{Co^{2+}}$ compared to $\langle\mu\rangle_{Mn^{2+}}$. Moreover, table 1 also shows that for the fluorines F(1), F(2), F(3), F(6), and F(7) (for which the M–F–M bond angles are nearly 180°), the non-axiality in the dipolar field is much smaller. On the other hand, for F(4), F(5), and F(8) (for which the M–F–M bond angles are far from 180°), the deviation from axial symmetry is significant, particularly for F(4) and F(8). Thus, from the results of table 1, we have divided the eight types of fluorine into six groups. In group 1 there is F(1), in group 2 there are F(2) and F(3), and in groups 3 and 4 there are F(4) and F(5) respectively. Group 5 consists of F(6) and F(7), and F(8) belongs to group 6. The experimental line is then fitted as a superposition of six different lines. As the numbers of fluorines belonging to each type, namely F(1), F(2), etc, are known from the structural data (table 1), we can associate a number belonging to each group as mentioned above. Using this knowledge, we have introduced the required restrictions on the area under each of the six lines used to fit the experimental spectrum.

Figure 3(a) shows the ^{19}F NMR experimental spectrum of $KCoFeF_6$ recorded at 34 MHz together with the theoretically fitted one at 294 K. All of the six lines used to fit the

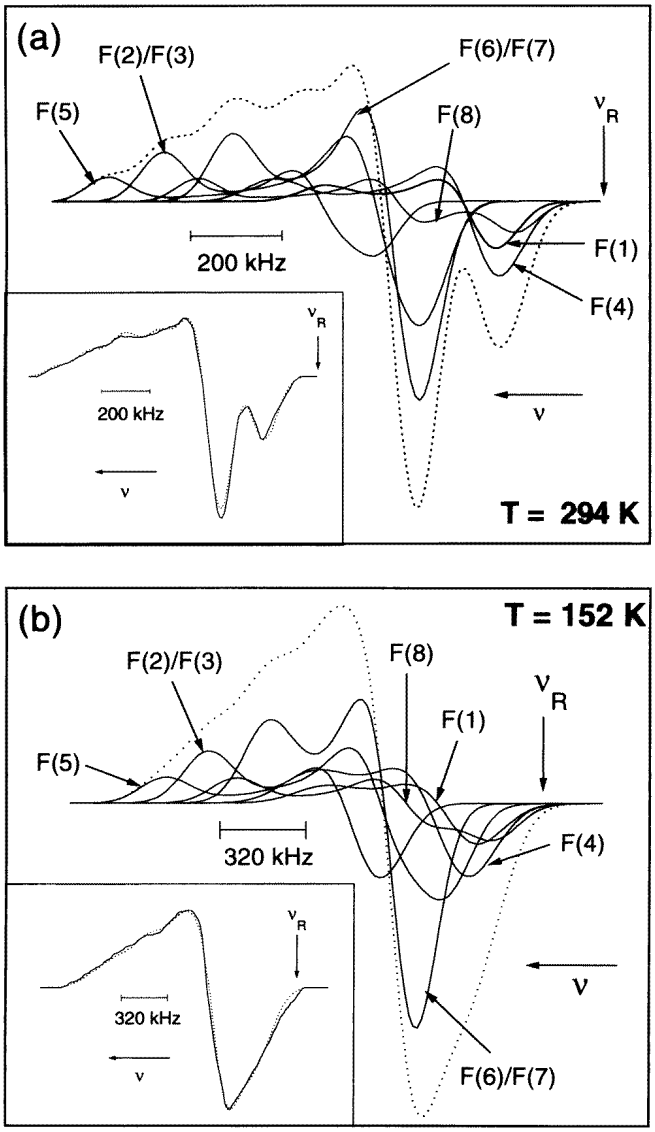

Figure 3. The theoretically generated ^{19}F NMR powder pattern (dotted curves) for $KMnFeF_6$, convoluted with six constituent lines (continuous curves) at (a) 294 K, (b) 152 K, and (c) 122 K. The numbers indicate the different groups of fluorines, as mentioned in the text. The resonance frequency is $\nu_R = 34$ MHz; the left-pointing arrow ($\leftarrow$) indicates the increasing direction of frequency, and the downward-pointing arrow ($\downarrow$) indicates the resonance position (ν_R) in the NH_4F solution. The inset of each figure shows the corresponding experimental ^{19}F NMR spectrum with the theoretically fitted powder pattern (dotted curves).

experimental line are also included. It may be seen that the composite experimental spectrum fits satisfactorily with the theoretical one. This supports the above consideration regarding the nature of the internal fields at different fluorine sites. The parameters used to obtain the best-fit spectrum at 34 MHz are also found to generate a spectrum satisfactorily close to the experimental data at 15 MHz.

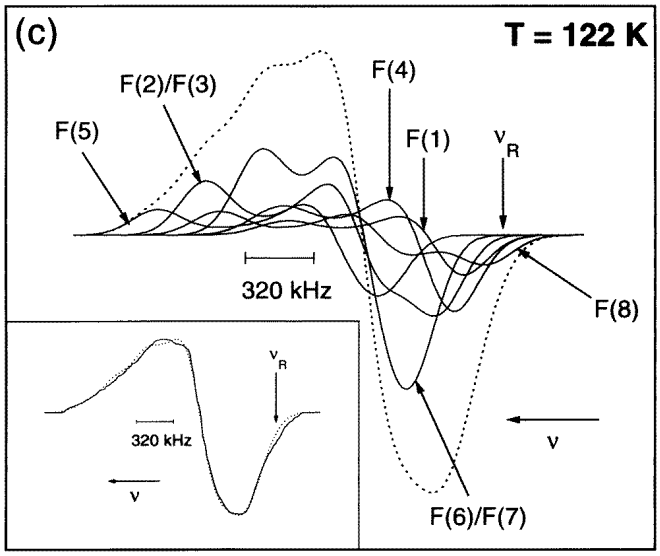

Figure 3. (Continued)

2.2. The shift parameters and linewidth at 294 K

Table 2 shows the principal components, namely K_1, K_2, and K_3, of the combined (hyperfine and dipolar) shift tensors of the fluorines corresponding to the six lines used to fit the experimental spectrum, as well as the normalized areas under each of the lines. The values of K_{iso}, K_{ax}, K_{aniso}, and the intrinsic linewidth, 2β (corrected for the contribution due to demagnetizing field), are also listed. By comparing the areas under each of the six lines with the numbers of fluorines of each type as well as the values of the shift parameters from tables 1 and 2, we have assigned each of the six lines to a particular type of fluorine. It is observed that the magnitude of K_{iso} (for the fluorines) is a minimum for F(1) and F(4) in the case of $KCoFeF_6$, whereas this occurs only for F(1) in the case of $KMnFeF_6$ [10]. As the dipolar field at the F(4) site is more anisotropic (table 1), the appearance of a structure towards the low-frequency side in $KCoFeF_6$ (figure 2(a)) may be a consequence of this fact. On the other hand, the value of K_{iso} is a maximum (for the fluorines) for F(5) for both compounds. The values of K_{iso} for different types of fluorine in table 2 provide an idea of the nature of

Table 2. The shift parameters and linewidths (2β) for $KCoFeF_6$ at 294 K.

Line	Fluorine	Normalized area	2β (kHz)[a]	K_1 (%)[b]	K_2 (%)[b]	K_3 (%)[b]	K_{iso} (%)	K_{ax}^{expt} (%)	K_{aniso}^{expt} (%)
1	F(1)	4.2	45.8	0.71	0.79	1.84	1.11	0.36	0.04
2	F(2)/F(3)	16.0	43.4	1.10	1.39	2.84	1.76	0.50	0.14
3	F(4)	8.1	51.5	0.68	0.87	2.05	1.21	0.42	0.09
4	F(5)	8.0	43.4	1.42	1.84	3.26	2.16	0.54	0.21
5	F(6)/F(7)	15.9	43.4	1.16	1.29	2.40	1.61	0.39	0.07
6	F(8)	8.3	43.4	0.58	1.26	2.57	1.47	0.55	0.34

[a] The estimated errors are less than ± 6.5.
[b] The estimated errors are less than ± 0.03.

the variation of the average M–F bond lengths (in the M–F–M′ bonds) for different types of fluorine in $KCoFeF_6$. Furthermore, it is to be noted that there is a considerable departure of the fitted linewidth 2β (after correction for the contribution due to the demagnetizing field) from that due to the nuclear contribution $\delta\nu_n$ (table 1). This was not observed in the case of $KMnFeF_6$. A possible reason for such a departure in the case of $KCoFeF_6$ may be the fluctuations of the contribution to the dipole and hyperfine fields arising from the 4b sites. As the magnetic moments of the two magnetic ions are different for $KCoFeF_6$ and almost the same for $KMnFeF_6$, the above-mentioned fluctuations would lead to a line broadening for the former.

2.3. Calculation of hyperfine coupling constants

K_{iso} in the case of $KCoFeF_6$ may be written as

$$K_{iso} = \frac{A_s^{Co^{2+}}\langle S_z\rangle^{Co^{2+}} + A_s^{Fe^{3+}}\langle S_z\rangle^{Fe^{3+}}}{\gamma\hbar H_R} \tag{5}$$

where, $A_s^{Co^{2+}}$ and $A_s^{Fe^{3+}}$ are the separate contributions of Co^{2+} and Fe^{3+} ions to the ^{19}F transferred hyperfine coupling constant for the fluorine belonging to the bond Co^{2+}–F–Fe^{3+}, and $\langle S_z\rangle = \chi_M H_R/Ng\mu_B$. If the value of $A_s^{Fe^{3+}}$ is taken from the calculated values of A_s for $KMnFeF_6$, we can estimate $A_s^{Co^{2+}}$ for $KCoFeF_6$. Here,

$$\langle S_z\rangle^{Co^{2+}} = \langle\mu\rangle_{Co^{2+}}/g\mu_B \qquad \langle S_z\rangle^{Fe^{3+}} = \langle\mu\rangle_{Fe^{3+}}/g\mu_B$$

and the values of $\langle\mu\rangle_{Fe^{3+}}$ and $\langle\mu\rangle_{Co^{2+}}$ are obtained using equation (4). The estimated values of $A_s^{Co^{2+}}$ and of $A_s^{Fe^{3+}}$ for the different fluorines in $KCoFeF_6$ are given in table 3. The values of $A_s^{Co^{2+}}$ in the present case are found to be close to those obtained for other fluoride compounds such as $KCoF_3$ [13, 14] and Co^{2+} in $KMgF_3$ [15]. An estimate of the spin densities in the 2s orbitals of F^- ions is made by using the relation

$$f_s = (S_{Co^{2+}}A_s^{Co^{2+}} + S_{Fe^{3+}}A_s^{Fe^{3+}})/A_{2s}.$$

The values of f_s are also listed in table 3. They provide a quantitative estimate of the variation of the amount of spin transfer from the 3d orbitals of Co^{2+} and Fe^{3+} to the 2s orbitals of the six types of fluorine in $KCoFeF_6$. A knowledge of this spin transfer would be useful for determining the strength of the superexchange interactions and how it varies among different bonds [16].

Table 3. The hyperfine coupling constants (A_s) and covalency parameters (f_s) for all of the fluorines in the case of $KCoFeF_6$.

Fluorine	$A_s^{Fe^{3+}}$ (10^{-4} cm^{-1})†	$A_s^{Co^{2+}}$ (10^{-4} cm^{-1})	f_s (%)
F(1)	17.4	8.3	0.48
F(2)/F(3)	18.2	24.4	0.87
F(4)	16.1	12.5	0.56
F(5)	20.5	32.2	1.09
F(6)/F(7)	17.1	21.8	0.79
F(8)	16.6	18.7	0.71

† As obtained for $KMnFeF_6$ (reference [10]).

2.4. Temperature dependence of the NMR spectrum

Figure 4 shows some typical ^{19}F NMR spectra for temperatures in the range $T_N < T \leqslant 400$ K for $KCoFeF_6$. A structure which is observed towards the low-frequency side at 294 K becomes more pronounced with the increase in temperature, whereas it becomes less pronounced with the lowering of temperature, and finally merges with the main line at around 230 K. The whole spectrum is found to shift slowly towards the high-frequency side with the decrease in temperature from 400 K, and the line finally vanishes at ∼110 K (T_N). This feature is quite different from what is observed in the case of $KMnFeF_6$ [11]. In this case the main line was shifted towards the high-frequency side up to 270 K, below which a structure appeared towards the high-frequency side. However, from below 200 K, the whole spectrum started to shift in the opposite direction (towards the low-frequency side, i.e. the reference position ν_R) compared to that for $KCoFeF_6$, until at T_N the whole line vanished. Thus a comparison of the spectral features for $KMnFeF_6$ and $KCoFeF_6$ reveals that introduction of the Co^{2+} ion (with anisotropic spin) in place of the Mn^{2+} ion significantly affects the behaviour of the local magnetic field around the ^{19}F sites, as a function of temperature, when the two systems approach T_N. On the other hand, the intrinsic linewidth for all of the constituent lines increases considerably below 160 K, whereas the bulk susceptibility does not show such extra enhancement in this region. The inset of figure 5(b) shows this feature for one of the fluorines. This observed

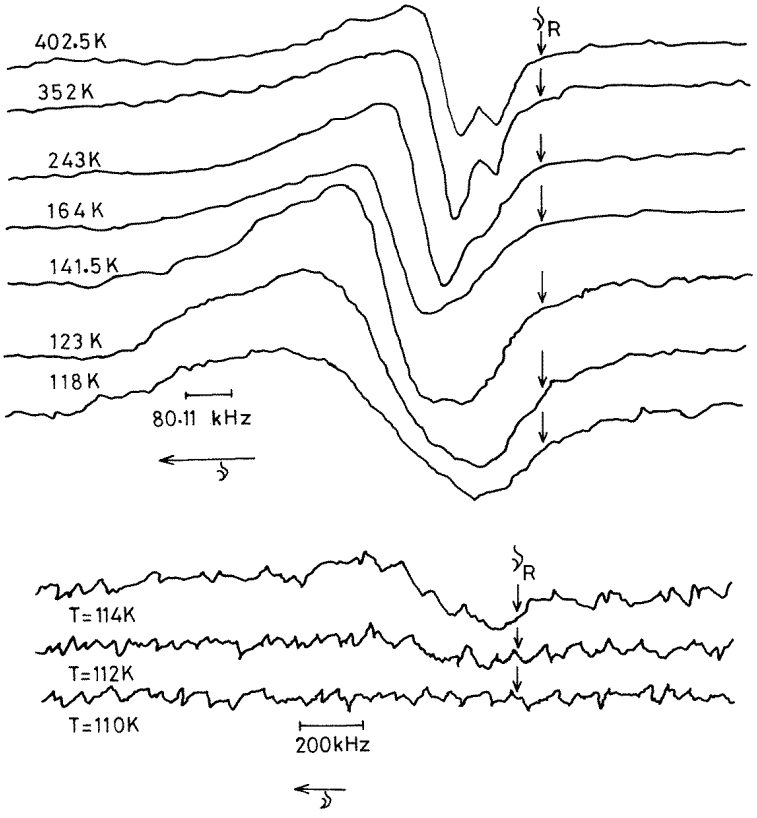

Figure 4. ^{19}F NMR spectra of polycrystalline $KCoFeF_6$ at 15 MHz for temperatures in the range $T_N \leqslant T \leqslant 400$ K, showing various features as T is varied, as described in the text.

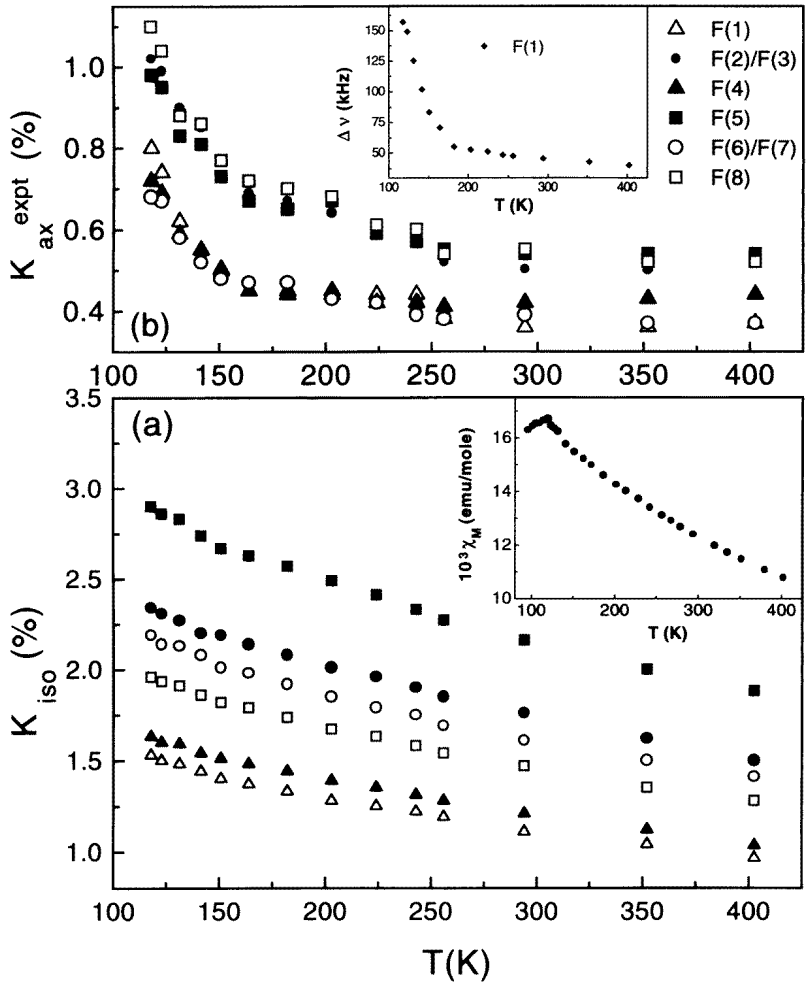

Figure 5. The temperature dependence of (a) the isotropic shifts (K_{iso}) and (b) the anisotropic shifts (K_{ax}) of different types of fluorine in $KCoFeF_6$. The inset in (a) shows the temperature variation of the molar susceptibility (χ_M) (reference [6]) at 6 kOe of this compound and the inset in (b) shows a plot of the temperature dependence of the intrinsic linewidth ($\Delta\nu$) of the constituent line corresponding to F(1).

feature resembles the effect of slowing down of the electron spin fluctuations on the ^{19}F NMR linewidth as T_N is approached.

Using the knowledge of the calculated dipolar field at 294 K (table 1), the experimental spectra obtained below this temperature are fitted theoretically using equation (1). The parameters which give the best-fit spectrum at 15 MHz are used to fit the spectrum at the same temperature recorded at 34 MHz. It is found that the spectrum at 34 MHz fits quite satisfactorily with very minor changes of these parameters, indicating the consistency of the fitting procedure. The principal components of the combined shift tensors K_1, K_2, K_3 for all of the lines are determined from the averages of the parameters used to fit the experimental line at 15 and 34 MHz at each temperature. Figures 3(b) and 3(c) show the theoretically generated ^{19}F NMR powder pattern for $KCoFeF_6$ at 34 MHz convoluted with six constituent lines at

152 K and 122 K. The inset in each case shows the experimental line with the theoretically fitted pattern. From this figure it is evident that the complex experimental spectra fit quite satisfactorily with the theoretically fitted one throughout the whole temperature range.

3. Discussion

3.1. The behaviour of the shift parameters with temperature

Figure 5 shows the variations of K_{iso} and K_{ax} as functions of temperature for all of the fluorines. In order to understand the nature of the variation of the local magnetic field (H_{local}) at a particular ^{19}F site as a function of temperature, it is necessary to determine the hyperfine contribution to the total shift parameters by subtracting the dipolar part at each temperature. As the dipolar shift tensor is traceless, its contribution to K_{iso} is zero. As a result the experimental K_{iso}–T curves show the behaviour of the isotropic part of H_{hyp} at each ^{19}F site as a function of temperature. However, the experimental values of K_{ax} and K_{aniso} contain both of the contributions, as mentioned above. For $KMnFeF_6$, the hyperfine contributions to the experimental K_{ax} and K_{aniso} were determined at each temperature [11]. However, in the case of $KCoFeF_6$ the assumption used for calculating $\langle\mu\rangle_{Fe^{3+}}$ in the dipolar-field calculation at 294 K cannot be used below the temperature where the χ_M^{-1}–T curves for $KMnFeF_6$ and $KCoFeF_6$ start to deviate from linearity. This is because the natures of these deviations for the two compounds are completely opposite in character, whereas $\langle\mu\rangle_{Fe^{3+}}$ is directly related to χ_M. Nevertheless, it may be seen from figure 5(b) that, from below 160 K, K_{ax} for each of the fluorines in $KCoFeF_6$ starts to increase significantly, though χ_M does not show such a sharp increasing trend below this temperature region. This suggests an enhancement of the anisotropic hyperfine field at all of the ^{19}F sites below 160 K. Such an enhancement in the local field anisotropy may be related to the nature of the antiferromagnetic ordering that appears below 110 K (T_N). Furthermore, it is seen that K_{iso} for each of the fluorines increases continuously up to 118 K (the temperature up to which the spectrum can be analysed), which is close to the antiferromagnetic ordering temperature T_N ($\sim$110 K) as observed from bulk susceptibility results [6]. Since the electron–nuclear hyperfine interaction is of very short range in nature, the respective parameters reveal information mainly about the local electronic susceptibility. As each of the fluorines is bonded on both sides with two magnetic ions, development of any short-range AF correlation among these ions below a certain temperature should be manifested as a decrease in K_{iso} with T. Such features are not observed in the temperature dependence of K_{iso} even up to 118 K. Thus the present result clearly shows the absence of any such correlation even up to 118 K, whereas in the case of $KMnFeF_6$ [11], which exhibits a ferrimagnetic transition at 148 K (T_N), the K_{iso}-values for the fluorines F(1)–F(4), and F(6) and F(7) decrease sharply from below 200 K (which is far above T_N) showing the signature of the development of short-range AF correlations. Thus a comparison of the behaviour of the K_{iso}–T curves for the two compounds clearly reveals that the development of short-range AF correlations is restricted even very close to T_N (within 8 K) in the paramagnetic region in the case of $KCoFeF_6$. This finding suggests that the effect of geometrical frustration present in the triangular lattice dominates over that of the tendency towards magnetic ordering in the square lattice in the case of $KCoFeF_6$ rather than that for $KMnFeF_6$. It may be mentioned that the strengths of the AF exchange interaction (indicated by the magnitude of the Curie–Weiss temperature, ~ -440 K) are almost the same for the two compounds. The present NMR results also suggest the absence of the development of any ferromagnetic (F) short-range correlation above T_N in $KCoFeF_6$ (i.e. a sharp increasing trend in K_{iso} with T below a certain temperature), whereas for $KMnFeF_6$ a clear signature of the development of F correlations was observed (in the ^{19}F NMR results) [11] from near $\sim$270 K

which is far above T_N (148 K). Nevertheless, it may be pointed out that the signature of F correlation was observed for $KCoFeF_6$ below T_N (110 K) in the χ_{ac}-measurement [8].

3.2. Isotropic shift versus bulk susceptibility

In the paramagnetic state, $K_{iso} = (zH_{hf}/N\mu_B)\chi_M$, where H_{hf} is the transferred hyperfine coupling constant, N is Avogadro's number, μ_B is the Bohr magneton, χ_M is the bulk molar susceptibility, and z is the number of nearest-neighbour magnetic ions bonded with the atom whose nucleus is being probed. Thus for a fixed value of H_{hf} the temperature dependence of

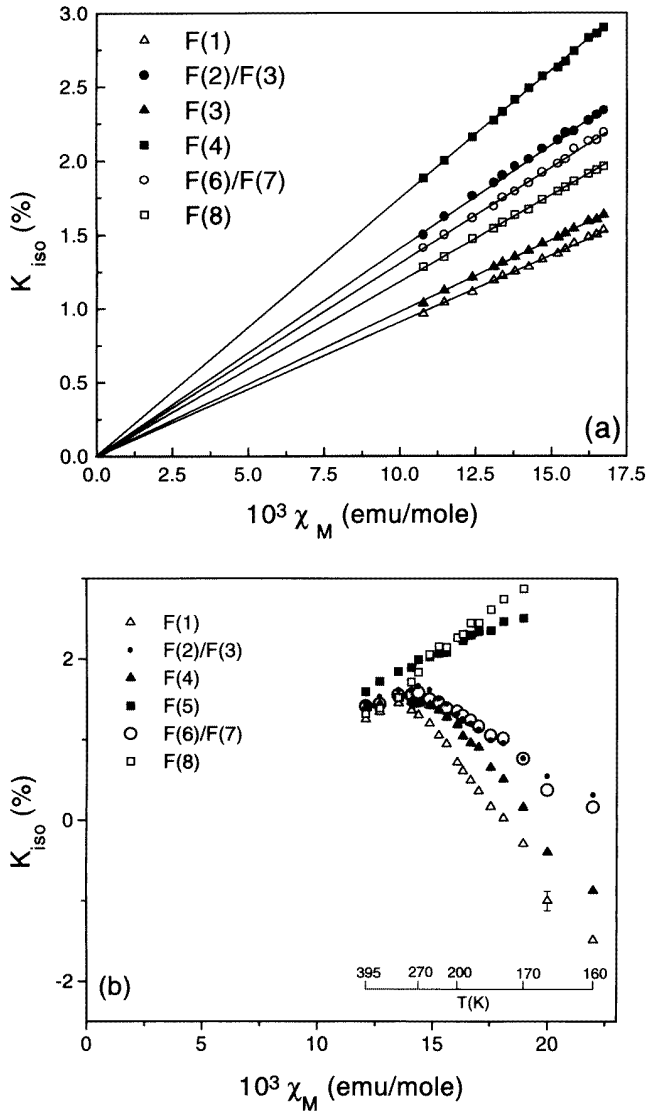

Figure 6. The variation of the isotropic shifts (K_{iso}) with the molar susceptibility (χ_M) in emu mol^{-1}, for different types of fluorine in (a) $KCoFeF_6$ and (b) $KMnFeF_6$ (reference [11]).

K_{iso} should be similar to that of χ_M with T in the paramagnetic region. Figure 6(a) shows the K_{iso}–χ_M plots for all fluorines in the case of $KCoFeF_6$ and figure 6(b) shows the same thing for $KMnFeF_6$. These plots clearly show the temperature dependence of the transferred hyperfine coupling. If a single mechanism dominates the temperature dependence of both the bulk susceptibility and the shift, the plot of K_{iso} versus χ_M should be a straight line passing through the origin. The slope of the line would give the value of H_{hf}. In the case of $KCoFeF_6$ the above plots, for all of the fluorines, are linear and pass through the origin throughout the whole temperature range T_N (110 K) $< T$ (118 K) $\leqslant$ 400 K, whereas in the case of $KMnFeF_6$ this occurs only in the range 270–395 K [11], showing the signature of a change in the hyperfine coupling constant below 270 K. The linear variation of K_{iso} versus χ_M throughout the whole temperature range for $KCoFeF_6$ thus suggests that the values of the coupling constants for all of the fluorines found at 294 K (table 3) remain the same throughout the whole temperature range mentioned above.

4. Conclusions

^{19}F NMR transferred hyperfine interaction parameters for eight types of fluorine in the unit cell of $KCoFeF_6$ are determined at 294 K. The values of these parameters provide an idea of the variation of average M–F bond lengths among the different types of fluorine. It is found that the nature of this variation is very similar to the corresponding previous findings for $KMnFeF_6$ [10]. The results also give an estimate of the fractional spin transfer from the 3d orbitals to the 2s orbitals of the different F^- ions.

The behaviour of K_{iso} with temperature in the range T_N (110 K) $< T$ (118 K) $\leqslant$ 400 K for $KCoFeF_6$ clearly suggests the absence of the development of any short-range AF correlation within the magnetic ions bonded with eight types of fluorine in the above temperature range, whereas this effect was very pronounced in the case of $KMnFeF_6$ from $\sim$270 K, which is far above T_N [11]. Thus the present findings from NMR for $KCoFeF_6$ suggest the dominance of geometrical frustration within the triangular lattice over the tendency of ordering of the magnetic ions belonging to the square lattice. Furthermore, the absence of the development of any short-range F correlation above T_N in $KCoFeF_6$ suggests that the spins in the triangular cycles in this case do not start to be canted from above T_N, as observed for $KMnFeF_6$. The results also indicate an appreciable increase in the anisotropic part of the local magnetic field at all ^{19}F sites below 150 K in $KCoFeF_6$. Thus a comparison of the present ^{19}F NMR results for $KCoFeF_6$ with those for $KMnFeF_6$ [11] reveals that the exact nature of the ordered state in $KCoFeF_6$ is still an open question, and needs detailed experiments on the ordered state using microscopic tools.

References

[1] Gaulin B D 1994 *Magnetic Systems with Competing Interactions (Frustrated Spin Systems)* ed H T Diep (Singapore: World Scientific) pp 286–326
Gingras M J P 1994 *Magnetic Systems with Competing Interactions (Frustrated Spin Systems)* ed H T Diep (Singapore: World Scientific) pp 238–85
[2] Ramirez A P 1994 *Annu. Rev. Mater. Sci.* **24** 453
[3] Hardy P A M, Hardy A and Ferey G 1973 *Acta Crystallogr.* B **29** 1654
[4] Banks E, Nakajima S and Williamson G J B 1979 *Acta Crystallogr.* B **35** 46
[5] Banks E, Shone M, Williamson R F and Boo W O J 1983 *Inorg. Chem.* **22** 3339
[6] Giri S, Ghoshray K and Ghoshray A 1995 *Solid State Commun.* **93** 493
[7] Giri S, Ghoshray K, Ranganathan R, Roy A, Bal B and Ghoshray A 1994 *Solid State Commun.* **91** 273
[8] Giri S and Ghoshray K 1998 *Phys. Rev.* B **57** 5198

[9] Owen J and Thornley J H M 1966 *Rep. Prog. Phys.* **29** 675
[10] Giri S, Ghoshray K, Ghoshray A and Chatterjee N 1996 *Phys. Rev.* B **54** 411
[11] Giri S, Ghoshray K, Ghoshray A and Chatterjee N 1997 *Phys. Rev.* B **56** 3347
[12] Bloembergen N and Rowland T J 1953 *Acta Mater.* **1** 731
[13] Tsang T 1964 *J. Chem. Phys.* **40** 729
[14] Thornley J H M, Windsor C G and Owen J 1965 *Proc. R. Soc.* A **284** 252
[15] Hall T P P, Hayes W, Stevenson R W H and Wilkens J 1963 *J. Chem. Phys.* **39** 35
[16] Kanamori J 1959 *J. Phys. Chem. Solids* **10** 87